Int. J. Multiphase Flow, Vol. 1, pp. 537–553. Pergamon Press, 1974. Printed in Great Britain.

A FLOW PATTERN MAP FOR GAS—LIQUID FLOW IN HORIZONTAL PIPES

J.M. MANDHANE, G.A. GREGORY and K. AZIZ

Department of Chemical Engineering, The University of Calgary, Calgary, Alberta (Canada)

(Received November 29, 1973)

Summary

Various flow pattern maps for two-phase gas—liquid flow in horizontal pipes are tested against the 5935 flow pattern observations presently contained in the UC Multiphase Pipe Flow Data Bank.

A new flow regime correlation representing an extension of the work done by Govier and Aziz [3] is presented and is shown to be in better agreement with the data than the other correlations tested. A computer program for this correlation is included.

It is also shown that there is no significant improvement obtained by including the effects of the physical properties of the fluids using any of the physical property parameters which have been proposed so far.

Introduction

Numerous studies [1, 2, 3] have shown that no single theory or correlation can satisfactorily predict the pressure gradient or liquid hold-up over all possible flow regimes encountered in two-phase gas—liquid flow in pipes. Although empirical correlation methods are still widely used, there is a growing trend toward the use and development of mechanistic models [3, 16, 17]. In either case it is important from the designer's point of view to be able to predict accurately what flow pattern will occur for given input flow rates, pipe size, and fluid properties. Only then can the proper flow model be selected. Many methods have been presented in the literature for this purpose, usually in the form of two-dimensional maps in which the locations of the boundaries between flow pattern regions are based on empirical observations. Many of these maps result from data covering a rather limited range of fluid properties and pipe diameters. Consequently, large discrepancies are often observed between a predicted flow regime and that actually observed in a subsequent test.

In this study, some commonly used maps are tested critically against data representing a very wide range of conditions, in most cases involving ten to twenty times the number of observations which were originally used to formulate the map. These test data are combined in a comprehensive data

bank which will be discussed later in this paper. The terms used here to designate the various flow patterns (*e.g.* stratified, slug, etc.) are consistent with the definitions used by Govier and Aziz [3]. As a consequence of the evaluation, a modified map is proposed which is simple to use and which is in overall better agreement with almost six thousand data points than any of the existing maps.

Previous work

Various flow pattern maps which have appeared in the literature are briefly discussed below in chronological order.

Bergelin and Gazley [4] suggested one of the first flow pattern maps. Their diagram, based on the air—water system in a 1-in. pipe, uses the liquid and gas mass flow rates, M_L and M_G, as the coordinates. Johnson and Abou-Sabe [5] proposed a flow pattern map which is very similar to that of Bergelin and Gazley and is based on air—water data in 0.87-in. pipe.

Alves [6] suggested a map based on data for air—water and air—oil mixtures in a 1-in. pipe utilizing the superficial liquid and gas velocities, V_{SL} and V_{SG}, as the coordinates. He was able to represent both of the systems on a single map.

Baker [7] proposed a flow pattern map based on the data of Jenkins [8], Gazley [9], Alves [6], and Kosterin [10]. Most of these data are for the air—water system. Baker plotted G/λ *versus* $L\lambda\psi/G$, which, for the air—water system, is equivalent to gas mass velocity, G, *versus* ratio of liquid to gas velocity, L/G. Here, λ and ψ are fluid property correction factors and are defined as:

$$\lambda = \left[\left(\frac{\rho_G}{0.075}\right)\left(\frac{\rho_L}{62.3}\right)\right]^{1/2} \tag{1}$$

and

$$\psi = \frac{73.0}{\sigma}\left[\left(\frac{\mu_L}{1.0}\right)\left(\frac{62.3}{\rho_L}\right)^2\right]^{1/3} \tag{2}$$

In eqns. (1) and (2), ρ_G and ρ_L have the units (lb./ft^3), μ_L has units of (centipoise) and σ is expressed in (dyne/cm).

White and Huntington [11] proposed a flow pattern map based on their data obtained in 1-, 1½-, and 2-in. pipes with gas—oil, air—oil and air—water systems. They used liquid and gas mass velocities, L and G, as the coordinates.

Hoogendoorn [12] used the mixture velocity, V_M, and the input gas volume fraction, C_G, as coordinates as first proposed by Kosterin [10] in a flow pattern map which is based on several air—oil and air—water systems. Hoogendoorn observed modest effects due to pipe diameter and liquid properties at liquid viscosity less than 50 cP. The coordinate system they used

results, however, in the crowding of important wave and annular-mist patterns into a very small area on the map.

Govier and Omer [13] presented a map based on their data for air—water system in a 1.026-in. pipe. The liquid and gas mass velocities, L and G, were used as the coordinates.

Scott [14] modified Baker's [7] diagram by making use of the more recent data of Hoogendoorn [12], and Govier and Omer [13]. The modified diagram does not have clearcut transition boundaries but instead shows relatively wide bands depicting regions of transition from one flow pattern to another.

Eaton *et al.* [15] obtained extensive data on natural gas—water, natural gas—crude oil, and natural gas—distillate systems in 2- and 4-inch pipes. They correlated the flow pattern observations on a map using as coordinates, a two-phase Reynolds number,

$$\mathrm{Re}_{tp} = \frac{M_M E_L^{\,2}}{D\mu_M} \tag{3}$$

and a two-phase Weber number,

$$\mathrm{We}_{tp} = D\left[\frac{\rho_L V_{SL}}{\sigma E_L^{\,1/2}} + \frac{\rho_G S^2 (1-E_L)^{1/2}}{\sigma}\right] \tag{4}$$

where

$$\mu_M = \mu_L E_L + \mu_G (1-E_L) \tag{5}$$

and

$$S = \frac{V_{SL}}{1-E_L} - \frac{V_{SL}}{E_L} \tag{6}$$

Note that the *in situ* liquid volume fraction, E_L, must be known in order to use the Eaton *et al.* map. Moreover, their definitions of flow patterns are somewhat different from those commonly found in the literature which results in apparent subdivisions of the usually defined regions. The data bank which is discussed shortly contains the Eaton *et al.* data, but the flow pattern observations have been interpreted according to the commonly accepted definitions.

Al-Sheikh *et al.* [1] have taken an entirely different approach to develop a method to predict flow pattern. Their correlation is based on the AGA—API Two-Phase Flow Data Bank referred to by Dukler *et al.* [2]. They use a total of 4475 data points and produce a complex correlation which requires a set of twelve figures on ten different coordinate systems. They did not attempt to define lines of separation between different flow patterns but have tried to enclose all of the data belonging to a particular pattern into a

closed region. It must be recognized that this effectively assumes all of the flow pattern observations are completely reliable. A sequential procedure is required to predict the flow pattern. Because the boundaries of their regions are highly irregular, this method is not readily suited for a computer oriented study.

Govier and Aziz [3] have presented a revised version of the Govier and Omer [13] flow pattern map. The revision is based on, in addition to the Govier and Omer data, the data of Baker [7] and Hoogendoorn [12], and others. The coordinate system for this revised diagram is also different from that originally used by Govier and Omer in that the superficial liquid and gas velocities, V_{SL} and V_{SG}, are used, as originally suggested by Alves [6].

Govier and Aziz also suggest that with suitable modification to the coordinates, the revised Govier and Omer map can be used with other than the air—water system. Specifically, these authors recommend that fluid property parameters, defined as

$$X = \left(\frac{\rho_G}{0.0808}\right)^{1/3} \quad Y \tag{7}$$

$$Y = \left[\left(\frac{\rho_L}{62.4}\right)\left(\frac{72.4}{\sigma}\right)\right]^{1/4} \tag{8}$$

be used to multiply the actual superficial fluid velocities as follows,

$$\tilde{V}_{SG} = X\, V_{SG} \tag{9}$$

$$\tilde{V}_{SL} = Y\, V_{SL} \tag{10}$$

In eqns. (7) and (8), ρ_L and ρ_G are expressed in (lb./ft^3), and σ has units (dyne/cm). $\tilde{V}_{SL}$ and $\tilde{V}_{SG}$ are then used in the normal way with the revised Govier and Omer map. This is referred to as the revised Govier and Omer map with physical property parameters. The quantities $\tilde{V}_{SL}$ and $\tilde{V}_{SG}$ thus represent "effective" superficial velocities for all systems except air—water; for the air—water system, they are the actual superficial velocities.

Two-phase flow data bank

The AGA—API Two-Phase Flow Data Bank as referred to by Dukler *et al.* [2] was the first available major compilation of data for two-phase flows in horizontal, vertical and inclined pipes. In 1970, a copy of this data bank was acquired by the present authors in the form of a magnetic tape. It then contained the equivalent of about 22,000 computer cards representing some 10,000 data points. These data had all been extracted from the literature available prior to 1962, and had been subjected to consistency tests and other culling procedures.

In formulating the present study, it was anticipated that this data bank would be used extensively and it was evident that repeated reading of the magnetic tape would be a major cost factor in any computer study. Consequently, the various formats specified for the data were carefully examined to determine whether or not it was possible to compress the tape without sacrificing any significant information.

It turned out that a reduction of almost 50% in the cost of reading the complete magnetic tape could be achieved without the loss of any significant information. Furthermore, the elimination of one card per data point has significantly reduced the work involved in adding new data to the tape.

The authors have updated the bank with research results published since 1962. Thus, over 4000 additional data points, mostly for horizontal flow, have been added, bringing the present total to over 14,000 points in all. It is intended that new data should continue to be included in the UC Multiphase Pipe Flow Data Bank as they are published or otherwise made available.

Scope of this study

For use in this study, all of the data for horizontal flow in which an observed flow pattern was recorded were separated from the main tape. This amounted to a total of 5,935 individual observations which can be used for testing purposes. The wide range of values for physical properties and flow parameters encompassed by these data is indicated in Table 1.

TABLE 1

Range of parameter values for data used in this study

Inside pipe diameter (D)	0.5—6.5 in.
Liquid phase density (ρ_L)	44.0—63.0 lb./ft^3
Gas phase density (ρ_G)	0.05—3.15 lb./ft^3
Liquid phase viscosity (μ_L)	0.30—90.0 centipoise
Gas phase viscosity (μ_G)	0.010—0.022 centipoise
Surface tension (σ)	24.0—103.0 dynes/cm
Superficial liquid velocity (V_{SL})	0.003—24.0 ft./s
Superficial gas velocity (V_{SG})	0.14—560 ft./s

A subset of the above data that is of interest, especially for comparing flow pattern maps, contains only those data relating to the air—water system. These air—water data were selected on the basis of the physical property constraints indicated in Table 2. The ranges are specified in order to account for pressure and temperature difference in the various studies represented. On this basis, a total of 1178 points were found for the air—water system.

In constructing his flow pattern map, Baker [7] used data from a number of studies, including those of Bergelin and Gazley [4] and Alves [6]. Since the Baker correlation is very widely used in the petroleum industry, it is of

TABLE 2

Range of parameter values used as criteria for air—water system

Liquid phase density (ρ_L)	60.0—65.0 lb./ft^3
Gas phase density (ρ_G)	0.065—0.090 lb./ft^3
Liquid phase viscosity (μ_L)	0.75—1.1 centipoise
Gas phase viscosity (μ_G)	0.017—0.02 centipoise
Surface tension (σ)	69.0—73.0 dyne/cm

particular interest to test this method against all of the 5,935 observations.

The flow pattern maps presented by Hoogendoorn [12] and Govier and Aziz [3] have both resulted from extensive data, representing a reasonably wide range of parameter values. Consequently, both were selected to be thoroughly investigated in this study.

Since the map of Eaton *et al.* [15] requires knowledge of the *in situ* hold-up, and furthermore, since the definitions these authors use for flow patterns are not consistent with those found elsewhere throughout the literature, their correlation was not included in the present comparison.

Scott's [14] modification of Baker's correlation is not treated separately, since it is very similar to the original Baker diagram except for his use of transition regions between flow patterns.

The diagram presented by White and Huntington [11] is limited to low liquid velocities and is not promising as an overall prediction device. It is therefore not included in this study.

As discussed above, the observations of Bergelin and Gazley [4] and Alves [6] have essentially been included in the consideration of Baker's flow pattern map. For this reason, the individual diagrams presented by those authors are not considered here.

The map of Johnson and Abou-Sabe [5] is based on data covering a very limited range; it was not included in this study.

Finally, due to its unwieldy nature, the correlation procedure of Al-Sheikh *et al.* [1] is also excluded.

Evaluation of existing flow pattern maps

The various diagrams under study were written into the computer program in terms of the original coordinate systems used by the authors. Two parameters, defined below, were calculated to facilitate comparisons.

$$\alpha_i = \left(\frac{\text{Number of points correctly predicted to lie in flow regime } i}{\text{Number of points which were observed in flow regime } i} \right) \times 100 \qquad (11)$$

Thus, α_i represents the percentage success of a given flow pattern map with respect to a particular flow regime.

$$\beta = \left(\frac{\text{Total number of observations correctly predicted to lie in their respective flow regimes}}{\text{Total number of observations}} \right) \times 100 \qquad (12)$$

β is thus the overall percentage success of a given flow pattern map.

Results of the comparison based on the air—water data are shown in Table 3. It should be noted that in Table 3 the bubble and elongated bubble (sometimes referred to as plug) flow regimes are grouped together as simply bubble flow. Also no distinction is drawn between annular and annular-mist flow. The region designated in this study as dispersed bubble is sometimes also referred to in the literature as froth flow.

TABLE 3

Comparison of flow pattern maps using air—water data

Flow pattern	Number of observations	Values of α		
		Baker	Hoogendoorn	Revised Govier—Omer
Bubble	12	58.4	91.6	58.4
Stratified	229	72.1	89.1	52.8
Wave	162	9.9	64.2	43.2
Slug	453	49.0	57.8	73.7
Annular-mist	320	97.5	94.1	95.0
Dispersed bubble	2	0.0	0.0	0.0
Total	1178			
β		61.3	74.9	71.0

The results of the comparison of flow pattern maps for all 5,935 observations are shown in Table 4.

It is interesting to note that while the fluid property corrections defined by eqns. (7) and (8) were expected to improve the reliability of the revised Govier and Omer map, in fact the reverse is true for most of the flow regimes.

It is also interesting to note the total failure of all of these maps to predict the dispersed bubble flow regime. In fact, there is some evidence that the data (at least the observation regarding flow pattern) are partly at fault. When all 5,935 points are plotted on V_{SL}, V_{SG} coordinates, a substantial number of the observations designated as "dispersed bubble" are seen to lie in the region of high gas rate and low liquid rates where one would normally expect annular-

TABLE 4

Comparison of flow pattern maps using all available data

Flow pattern	Number of observations	Values of α			
		Baker	Hoogendoorn	Revised Govier—Omer	Revised Govier—Omer with physical property parameters
Bubble	758	20.4	64.6	32.4	23.3
Stratified	397	54.7	80.9	51.6	46.3
Wave	783	16.0	41.5	17.5	16.5
Slug	2020	24.0	58.7	63.4	58.6
Annular-mist	1746	84.7	90.5	91.0	93.2
Dispersed bubble	231	2.2	0.0	0.0	0.0
Total	5935				
β		41.5	65.7	58.3	55.6

mist flow to predominate. In any case, this flow pattern designation represents less than 4% of the total data and its importance will not be overstated here.

All of the maps do very well with respect to the annular-mist flow regime, whereas without exception they tend to predict wave flow very poorly. For all maps, there is evidence that the boundary between dispersed bubble and slug flow is located at a liquid flow rate that is too low. From the calculated values of β, it is apparent that the map presented by Hoogendoorn [12] is substantially more reliable than that of Baker [7], which has been used extensively, both in literature and in industrial design calculations.

Proposed flow pattern map

Following the examination of the flow pattern maps from the literature, it appeared that certain improvements could be made.

In the interests of simplicity, it was decided to generate a basic flow pattern map based on air—water data, and then attempt to apply physical property corrections. While this is certainly not a new approach, previous workers have not had access to the amount of data that were available for this study.

In all the previous attempts to apply physical property corrections to a base diagram, the axes of the diagram were modified. This approach shifts the flow regime boundaries for non-air—water data in only one direction. Another approach, which has not been used so far, is to shift specific transition boundaries according to some scheme. This is equivalent to assuming

that the effect of changes in a particular physical property may be different for different ranges of the flow rates of the two phases.

Another major decision involves the selection of the coordinate axes. There does not seem to be any reason to use complex and difficult-to-calculate parameters when it is apparent from the Govier and Aziz studies that the superficial phase velocities represent reasonable discrimination criteria. The choice was thus made to base the diagram on a log—log plot using V_{SL} and V_{SG} as the coordinate axes.

The proposed flow pattern map is shown in Fig. 1. The transition boundaries indicated were located primarily on the basis of a log V_{SL} *vs.* log V_{SG} plot of the 1178 flow pattern observations for the air—water system. However, where a reasonably distinct transition line was not obvious, reference was made to a second similar plot containing all 5,935 flow pattern observations from the data bank. Unfortunately, neither of these two data plots can be reduced in size with sufficient clarity to be included here. Coordinates for the transition boundaries shown in Fig. 1 are given in Table 5.

It is of interest to examine the relationship between the boundaries of the map proposed in this study and those of the other maps which have been discussed. In Fig. 2, the Baker, Hoogendoorn and revised Govier—Omer maps have been superimposed on the map shown in Fig. 1. In order to translate the Baker and Hoogendoorn maps to the log V_{SL}—log V_{SG} axes, the physical

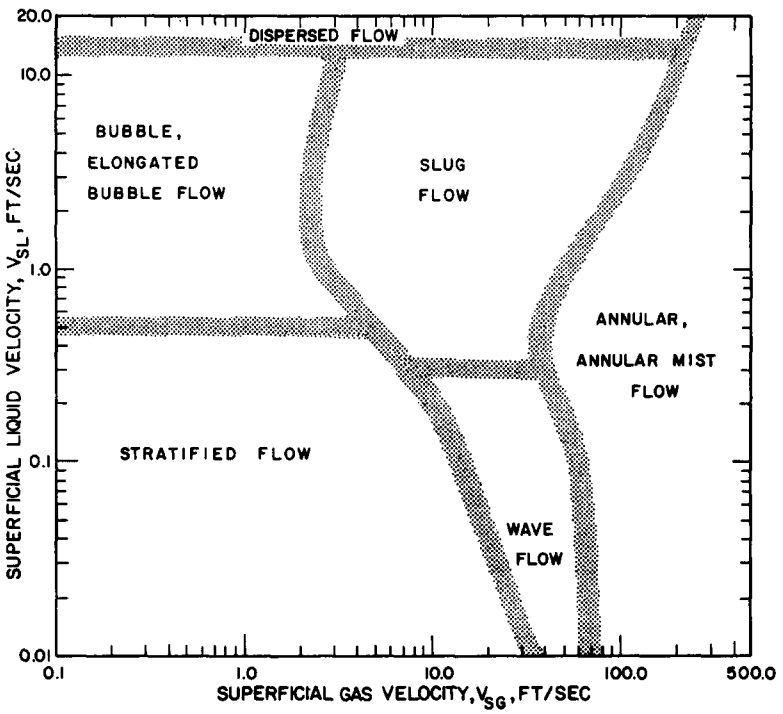

Fig. 1. Proposed flow pattern map.

TABLE 5

Coordinates for transition boundaries of proposed flow pattern map*

Transition boundary	V_{SG} (ft./s)	V_{SL} (ft./s)	Physical property correction — multiply equation of transition boundary by
Stratified to elongated bubble	0.1 5.0	0.5 0.5	$1.0/Y$
Wave to slug	7.5 40.0	0.3 0.3	Y
Elongated bubble and slug to dispersed bubble	0.1 230.0	14.0 14.0	Y
Stratified and elongated bubble to wave and slug	35.0 14.0 10.5 2.5 2.5 3.25	0.01 0.1 0.2 1.15 4.8 14.0	X
Wave and slug to annular-mist	70.0 60.0 38.0 40.0 50.0 100.0 230.0	0.01 0.1 0.3 0.56 1.0 2.5 14.0	X
Dispersed bubble to annular-mist	230.0 269.0	14.0 30.0	X

*To be plotted on log—log scale.

properties of the air—water system and a 1-in.-diameter pipe were assumed. It is perhaps not surprising to see that the proposed map is essentially an "average" of the other three.

One might argue on physical grounds that there should not be an apparent discontinuity in the superficial liquid velocity as indicated between the elongated bubble to stratified flow transition line and the slug to wave flow transition line. While this might be true for a single specific system, it must be remembered that (a) the transition boundaries should more correctly be viewed as transition regions, and (b) the diagram presented represents an average compromise over a wide variety of combinations of physical properties and pipe diameters.

There did not appear to be any direct procedure for devising the physical property parameters. As a first step, the air—water data were sorted according

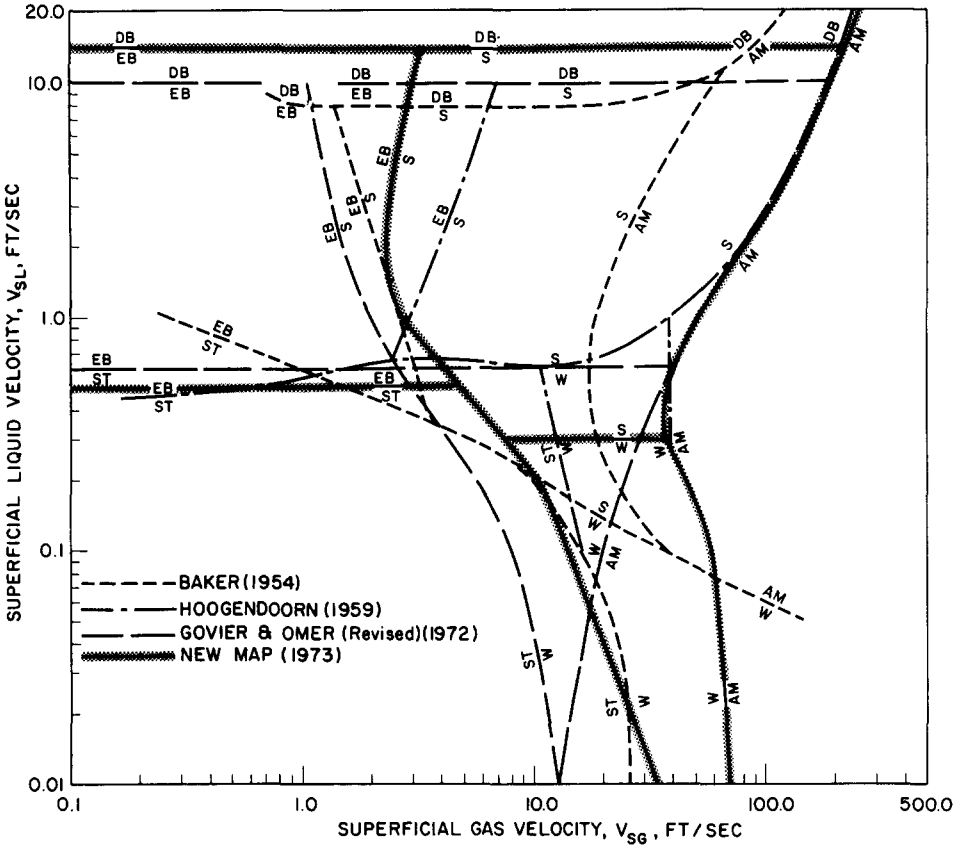

Fig. 2. Comparison of proposed flow pattern map with others used in this study. EB Bubble, elongated bubble flow; ST Stratified flow; W Wave flow; S Slug flow; AM Annular, annular-mist flow; DB Dispersed bubble flow.

to pipe diameter to investigate any possible effect of this variable. Although the resulting groups of data were too small to permit firm conclusions to be drawn, there was no observable diameter effect for pipe diameters greater than one inch. Any effect which actually does exist is masked by being included in the calculation of the superficial velocities.

As a starting point the physical property factors defined by eqns. (7) and (8) were used. All of the possible directional effects were evaluated for the various flow pattern boundaries. Various perturbations on the exponents used in the parameter definitions were then tried and finally, a viscosity effect was added. The final form of the physical property parameters is expressed as follows:

$$X' = \left(\frac{\rho_G}{0.0808}\right)^{0.2} \left(\frac{\rho_L}{62.4}\ \frac{72.4}{\sigma}\right)^{0.25} \left(\frac{\mu_G}{0.018}\right)^{0.2} \tag{13}$$

$$Y' = \left(\frac{\mu_L}{1.0}\right)^{0.2} \left(\frac{\rho_L}{62.4} \quad \frac{72.4}{\sigma}\right)^{0.25} \tag{14}$$

where ρ_G and ρ_L are expressed in lb./ft^3, μ_L and μ_G are expressed in centipoise, and σ has units of dyne/cm. These factors are applied to the flow pattern boundaries rather than to the axes of the map. The transition boundary can be defined using the coordinates specified in Table 5, in the form,

$$V_{SL} = \xi(V_{SG}) \tag{15}$$

To correct for physical properties, the right hand side of eqn. (15) is multiplied by the appropriate factor as specified in the last column of Table 5.

The proposed map, and the physical property correction procedure were then compared with the observations from the data bank, with the results shown in Table 6.

It is somewhat surprising to note the relatively small effect of the physical property parameters. In most circumstances one is obviously justified in ignoring them altogether. Comparing Table 6 with Tables 3 and 4, it can be noted that the proposed map is in substantially better agreement with the air—water data than any of the others tested, and it is in slightly better agreement with the overall data. While other forms of physical property factors could certainly have been chosen, it is doubtful if any criteria can be determined which will show a significantly greater success level, yet still retain the

TABLE 6

Comparison of proposed flow pattern map with available data

Air—water data			All data		
Flow pattern	Number of observations	Values of α for proposed base diagram	Number of observations	Values of α for proposed base diagram	Values of α for proposed base diagram with physical property parameters
Bubble	12	83.3	758	50.5	64.5
Stratified	229	78.6	397	72.5	73.0
Wave	162	71.6	783	50.2	55.2
Slug	453	79.7	2020	71.4	73.9
Annular-mist	320	92.8	1746	84.8	76.9
Dispersed bubble	2	0.0	231	0.0	0.0
Total	1178		5935		
β		81.8		67.2	68.2

desirable simplicity of a single two-dimensional map. It must also be remembered that assigning a flow regime label to a given flow condition is not an exact procedure and is based on a visual interpretation. It is thus a subjective judgement on the part of the investigator, which is particularly true when the flow is in a transition between two or more flow regimes.

As a final check for possible diameter effect on flow pattern, the 5,935 observations were divided into three diameter ranges and values of α and β were determined as before. The results are shown in Table 7. Clearly, the

TABLE 7

Effect of pipe diameter on agreement of data with proposed flow pattern map

Flow pattern	$D < 2.000''$		$2.000'' \leq D < 4.000''$		$D \geq 4.000''$	
	Number of observations	α	Number of observations	α	Number of observations	α
Bubble	422	69.7	166	46.4	170	69.4
Stratified	162	74.1	163	73.0	72	70.8
Wave	585	63.2	102	52.0	96	10.4
Slug	1431	70.9	265	79.6	324	82.4
Annular-mist	1512	80.1	224	59.4	10	0.0
Dispersed bubble	94	0.0	75	0.0	62	0.0
Total	4206 (70.9%)		995 (16.8%)		734 (12.3%)	
β	71.6		59.6		60.8	

proposed map tends to be more successful with data from small diameter pipes (less than 2 inches). This is not too surprising considering that approximately 70% of the flow pattern observations in the data bank are in this category. However, the overall success level of about 60% for the larger diameters still compares favorably with the overall success levels of the other maps for all the data (see Table 4). The proposed map has a significant advantage over the other maps when only the "larger than 4 inch" data are considered. In this case, the β-value of 60.8 for the proposed map compares with 15.0 for Baker, 55.6 for Hoogendoorn, and 45.5 for the revised Govier–Omer map. Furthermore, in the larger diameter ranges, the proposed map is very successful (about 80%) in the important slug flow regime. It is clear, however, that more flow pattern observations from large diameter systems are required for a thorough investigation of diameter effects.

A Fortran computer program, based on the proposed map (including the physical property factors), is given in the Appendix. This program can be used to predict flow patterns resulting from given input flow rates, fluid properties and pipe diameter for gas–liquid flow in horizontal pipes.

Conclusions

The commonly used flow pattern maps have been compared using extensive data which cover a wide range of physical properties and flow parameters. The diagram presented by Hoogendoorn [12] is shown to be the most reliable of those selected from the literature to be tested.

A new flow pattern map, representing an extension of the work of Govier and Aziz [3], is presented which is in substantially better agreement with air—water data than any other, and is slightly better than the Hoogendoorn diagram for all available data. Because of its simplicity, it is well suited to either computer or hand calculations.

The effect of pipe diameter appears to be adequately taken into account by using the superficial velocities, V_{SL} and V_{SG}, as the coordinate axes.

At the present time, no method exists for including the effect of the physical properties of the fluids which yields a significant improvement in flow pattern prediction. It is concluded that errors in the positions of the transition boundaries on a V_{SL} *vs.* V_{SG} diagram almost eliminated whatever physical property effects which may exist.

The designation of existing observations in the two-phase flow data bank as "dispersed bubble" should be considered suspect at the present time. As more data become available for this flow regime, a decision can be made regarding the validity of that allocation.

Acknowledgements

One of us (JMM) is grateful for the financial support received in the form of a Province of Alberta Graduate Fellowship. Financial support for this study has also been received from the National Research Council of Canada and The Petroleum Aid to Education Fund. The technical assistance of Mrs. M. Fogarasi has been much appreciated. Finally we wish to thank Dr. G.W. Govier for his helpful suggestions and comments on the results of this study.

Nomenclature

C_G	volume fraction of gas in the input mixture
D	pipe diameter (L)
E_L	*in situ* liquid volume fraction
G	mass velocity of the gas phase (M/L^2T)
L	mass velocity of the liquid phase (M/L^2T)
M_G	mass flow rate of the gas phase (M/T)
M_L	mass flow of the liquid phase (M/T)
M_M	($M_L + M_G$), the total mass flow rate (M/T)
S	slip velocity (L/T)
V_{SG}	superficial gas velocity (L/T)
V_{SL}	superficial liquid velocity (L/T)

V_M	$(V_{SL} + V_{SG})$, the mixture velocity, (L/T)
α	percent success in predicting a particular flow pattern, defined by eqn. (11)
β	percent success in overall predictions for a particular map, defined by eqn. (12)
λ	Baker's fluid property correction factor, defined by eqn. (1)
μ_G	viscosity of the gas phase at operating conditions (M/LT)
μ_L	viscosity of the liquid phase at operating conditions (M/LT)
μ_M	mixture viscosity (M/LT)
ρ_G	density of the gas phase at operating conditions (M/L^3)
ρ_L	density of the liquid phase at operating conditions (M/L^3)
σ	interfacial tension (F/L)
ψ	Baker's fluid property correction factor, defined by eqn. (2)

References

1 J.N. Al-Sheikh, D.E. Saunders and R.S. Brodkey, Can. J. Chem. Eng., 48 (1970) 21.
2 A.E. Dukler, M. Wicks and R.G. Cleveland, AIChE J., 10 (1964) 44.
3 G.W. Govier and K. Aziz, The Flow of Complex Mixtures in Pipes, Van Nostrand-Reinhold, New York, 1972, p.503.
4 O.P. Bergelin and C. Gazley, Proc. Heat Transfer and Fluid Mechanics Inst., May 1949, p.5.
5 H.A. Johnson and A.H. Abou-Sabe, Trans. A.S.M.E., 74 (1952) 977.
6 G.E. Alves, Chem. Eng. Progr., 50 (1954) 449.
7 O. Baker, Oil and Gas J., 53 (1954) 185.
8 R. Jenkins, M.S. Thesis, Univ. of Delaware, 1947.
9 C. Gazley, Ph.D. Thesis, Univ. of Delaware, 1949.
10 S.I. Kosterin, Izv. Akad. Nauk. S.S.S.R., Otd. Tekh. Nauk., No. 12, 1949, pp.1824.
11 P.D. White and R.L. Huntington, The Petrol. Eng., 27(9) (1955) D40.
12 C.J. Hoogendoorn, Chem. Eng. Sci., 9 (1959) 205.
13 G.W. Govier and M.M. Omer, Can. J. Chem. Eng., 40 (1962) 93.
14 D.S. Scott, in Advances in Chemical Engineering, Vol. 4, Academic Press, New York, 1963, p. 200.
15 B.A. Eaton, D.E. Andrews, C.R. Knowles, I.H. Silberberg and K.E. Brown, J. Petrol. Technol., 19 (1967) 815.
16 M.G. Hubbard and A.E. Dukler, paper presented at 65th Nat. Mtg. of A.I.Ch.E., Tampa, Fla., May 1968.
17 S.S. Agrawal, G.A. Gregory and G.W. Govier, Can. J. Chem. Eng., 51 (1973) 280.

APPENDIX

COMPUTER PROGRAM LISTING FOR PROPOSED FLOW PATTERN CORRELATION

```
      PROGRAM REGION(INPUT,OUTPUT)
C
C         THIS PROGRAM CALCULATES THE FLOW PATTERN REGION FOR ANY TWO
C         COMPONENTS FLOWING COCURRENTLY IN A PIPE, ACCORDING TO FLOW
C         PATTERN MAP OF MANDHANE, GREGORY, AND AZIZ.
C
C         INPUT DATA
C              VSL=SUPERFICIAL LIQUID VELOCITY, FT/SEC
C              VSG=SUPERFICIAL GAS VELOCITY, FT/SEC
C              DENSL=DENSITY OF LIQUID, LBM/CU.FT.
C              DENSG=DENSITY OF GAS, LBM/CU.FT.
C              AMUL=VISCOSITY OF LIQUID, CENTIPOISE
C              AMUG=VISCOSITY OF GAS, CENTIPOISE
C              SIGMA=INTERFACIAL TENSION, DYNES/CM.
C
  100 FORMAT(7F10.5)
  101 FORMAT(10X,≠PREDICTED FLOW PATTERN:  ELONGATED BUBBLE≠)
  103 FORMAT(10X,≠PREDICTED FLOW PATTERN:  STRATIFIED≠)
  105 FORMAT(10X,≠PREDICTED FLOW PATTERN:  WAVE≠)
  107 FORMAT(10X,≠PREDICTED FLOW PATTERN:  SLUG≠)
  109 FORMAT(10X,≠PREDICTED FLOW PATTERN:  ANNULAR MIST≠)
  111 FORMAT(10X,≠PREDICTED FLOW PATTERN:  DISPERSED BUBBLE≠)
  112 FORMAT(    10X,≠SUPERFICIAL LIQUID VELOCITY,FT/SEC = ≠,F10.5/10X,
     1≠SUPERFICIAL GAS VELOCITY,FT/SEC     = ≠,F10.5/10X,≠DENSITY OF LIQU
     2ID,LBM/CU.FT.        = ≠,F10.5/10X,≠DENSITY OF GAS,LBM/CU.FT.
     3     = ≠,F10.5/10X,≠VISCOSITY OF LIQUID,CENTIPOISE      = ≠,F10.5/
     410X,≠VISCOSITY OF GAS,CENTIPOISE         = ≠,F10.5/10X,≠INTERFACIAL
     5 TENSION,DYNES/CM.       = ≠,F10.5/10X,≠X1 CORRECTION
     6         = ≠,F10.5/10X,≠Y1 CORRECTION                        = ≠,
     7F10.5//)
  113 FORMAT(1H1,9X,≠CALCULATIONS ACCORDING TO FLOW PATTERN MAP OF≠/
     119X,≠MANDHANE, GREGORY, AND AZIZ≠)
      PRINT 113
      READ 100,VSL,VSG,DENSL,DENSG,AMUL,AMUG,SIGMA
      X1=((DENSG/0.0808)**0.333)*((DENSL*72.4/(62.4*SIGMA))**0.25)*
     1((AMUG/0.018)**0.2)
      Y1=((DENSL*72.4/(62.4*SIGMA))**0.25)*((AMUL/1.0)**0.2)
      PRINT 112,VSL,VSG,DENSL,DENSG,AMUL,AMUG,SIGMA,X1,Y1
      IF(VSL.LT.14.0*Y1)GO TO 114
      IF(VSG.LE.(230.0*((VSL/14.0)**0.206)*X1))GO TO 150
      GO TO 148
  114 IF(VSL.LE.0.1 )GO TO 122
      IF(VSL.LE.0.2 )GO TO 120
      IF(VSL.LE.1.15)GO TO 118
      IF(VSL.LE.4.8 )GO TO 116
      Y1345=2.5*(VSL/4.8)**0.248
      GO TO 126
  116 Y1345=2.5
      GO TO 126
  118 Y1345=10.5*(VSL/0.2)**(-0.816)
      GO TO 126
  120 Y1345=14.0*(VSL/0.1)**(-0.415)
      GO TO 126
  122 Y1345=14.0*(VSL/0.1)**(-0.368)
```

```
126 IF(VSL.LE.0.1 )GO TO 136
    IF(VSL.LE.0.3 )GO TO 134
    IF(VSL.LE.0.56)GO TO 132
    IF(VSL.LE.1.0 )GO TO 130
    IF(VSL.LE.2.5 )GO TO 128
    Y456=100.0*(VSL/2.5)**0.463
    GO TO 138
128 Y456=50.0*(VSL/1.0)**0.756
    GO TO 138
130 Y456=40.0*(VSL/0.56)**0.385
    GO TO 138
132 Y456=38.0*(VSL/0.3)**0.0813
    GO TO 138
134 Y456=60.0*(VSL/0.1)**(-0.415)
    GO TO 138
136 Y456=70.0*(VSL/0.01)**(-0.0675)
138 Y45=0.3*Y1
    Y31=0.5/Y1
    Y1345=Y1345*X1
    Y456=Y456*X1
    IF(VSG.LE.Y1345.AND.VSL.GE.Y31)GO TO 140
    IF(VSG.LE.Y1345.AND.VSL.LE.Y31)GO TO 142
    IF(VSG.GE.Y1345.AND.VSG.LE.Y456.AND.VSL.GT.Y45)GO TO 146
    IF(VSG.GE.Y1345.AND.VSG.LE.Y456.AND.VSL.LE.Y45)GO TO 144
    GO TO 148
140 PRINT 101
    GO TO 152
142 PRINT 103
    GO TO 152
144 PRINT 105
    GO TO 152
146 PRINT 107
    GO TO 152
148 PRINT 109
    GO TO 152
150 PRINT 111
152 STOP
    END
```

TYPICAL OUTPUT LISTING

```
CALCULATIONS ACCORDING TO FLOW PATTERN MAP OF
        MANDHANE, GREGORY, AND AZIZ
SUPERFICIAL LIQUID VELOCITY,FT/SEC =    1.00000
SUPERFICIAL GAS VELOCITY,FT/SEC    =   10.00000
DENSITY OF LIQUID,LBM/CU.FT.       =   55.00000
DENSITY OF GAS,LBM/CU.FT.          =     .04000
VISCOSITY OF LIQUID,CENTIPOISE     =    5.00000
VISCOSITY OF GAS,CENTIPOISE        =     .01000
INTERFACIAL TENSION,DYNES/CM.      =   65.00000
X1 CORRECTION                      =     .70027
Y1 CORRECTION                      =    1.37339


PREDICTED FLOW PATTERN:  SLUG
```